

Dalton Transactions

Accepted Manuscript



This is an *Accepted Manuscript*, which has been through the Royal Society of Chemistry peer review process and has been accepted for publication.

Accepted Manuscripts are published online shortly after acceptance, before technical editing, formatting and proof reading. Using this free service, authors can make their results available to the community, in citable form, before we publish the edited article. We will replace this *Accepted Manuscript* with the edited and formatted *Advance Article* as soon as it is available.

You can find more information about *Accepted Manuscripts* in the [Information for Authors](#).

Please note that technical editing may introduce minor changes to the text and/or graphics, which may alter content. The journal's standard [Terms & Conditions](#) and the [Ethical guidelines](#) still apply. In no event shall the Royal Society of Chemistry be held responsible for any errors or omissions in this *Accepted Manuscript* or any consequences arising from the use of any information it contains.

Barium borohydride chlorides;

Synthesis, crystal structures and thermal properties

Elisabeth Grube^a, Cathrine H. Olesen^a, Dorthe B. Ravnsbæk^{b*}, Torben R. Jensen^a

^a Center for Materials Crystallography, Interdisciplinary Nanoscience Center and Department of Chemistry, Aarhus University, Langelandsgade 140, 8000 Aarhus C, Denmark

^b Department of Physics, Chemistry and Pharmacy, University of Southern Denmark, Campusvej 55, 5230 Odense M, Denmark

*Corresponding author:

Dorthe B. Ravnsbæk

E-mail: dbr@sdu.dk

Abstract

Here we report the synthesis, mechanism of formation, characterization and thermal decomposition of new barium borohydride chlorides prepared by mechanochemistry and thermal treatment of MBH_4-BaCl_2 , $M = Li, Na$ or K in ratios 1:1 and 1:2. Initially, orthorhombic barium chloride, $o-BaCl_2$ transforms to $o-Ba(BH_4)_xCl_{2-x}$, $x \sim 0.15$. Excess $LiBH_4$ leads to continued anion substitution and a phase transformation to hexagonal barium borohydride chloride $h-Ba(BH_4)_xCl_{2-x}$, which accommodate higher amounts of borohydride, possibly $x \sim 0.85$ and resembles $h-BaCl_2$. Thus, two solid solutions are in equilibrium during mechano-chemical treatment of $LiBH_4-BaCl_2$ (1:1) whereas $LiBH_4-BaCl_2$ (2:1) converts to $h-Ba(BH_4)_{0.85}Cl_{1.15}$. Upon thermal treatment at $T > \sim 200$ °C, $h-Ba(BH_4)_{0.85}Cl_{1.15}$ transforms to another orthorhombic barium borohydride chloride compound, $o-Ba(BH_4)_{0.85}Cl_{1.15}$, which is structurally similar to $o-BaBr_2$. The samples with $M = Na$ and K has lower reactivity and form $o-Ba(BH_4)_xCl_{2-x}$, $x \sim 0.1$ and a solid solution of sodium chloride dissolved in solid sodium borohydride, $Na(BH_4)_{1-x}Cl_x$, $x = 0.07$. The new compounds and reaction mechanisms are investigated using in situ synchrotron radiation powder X-ray diffraction (SR-PXD), Fourier transformed infrared spectroscopy (FT-IR) and simultaneous thermogravimetric analysis (TGA) differential scanning calorimetry (DSC), mass spectroscopy (MS) and temperature programmed photographic analysis (TPPA).

1 Introduction

Renewable energy is an environmentally friendly alternative to fossil fuels, however, unevenly distributed over time and geographically. Therefore, a suitable energy carrier is needed to match the oscillating production and demand for energy.¹ Hydrogen has been proposed as a potential energy carrier due to high gravimetric energy density.² However, hydrogen is a gas at ambient conditions and challenging to store in a compact way, therefore, solid state hydrogen storage with promising hydrogen storage densities is considered.^{2,3} A wide range of new borohydride-based materials have attracted considerable interest during the past decade mainly because the low mass of boron and the high amount of hydrogen makes the BH_4^- complex anion an ideal building unit for rational design of novel metal borohydrides for hydrogen storage.³⁻⁶ Light metal borohydrides, *e.g.* LiBH_4 and $\text{Mg}(\text{BH}_4)_2$, have high gravimetric and volumetric hydrogen densities.^{7,8} Based on these many new bi- and tri-metallic borohydrides were discovered in the past few years involving many different metals and compositions, *e.g.* *s*-, *d*- and *f*-block metals, such as Sc, Y, Zn etc.^{2,7-13} Extreme structural and compositional flexibility within this class of materials has led to series of perovskite type materials, new ion conductors and the first porous hydrides.^{9,14-17}

One drawback of solid-state hydrogen storage is that reversible hydrogen release and uptake is often hampered by high thermodynamic stability, slow kinetics and requirement of high temperatures, often several hundred degrees Celsius. Reactive hydride composites have proven successful, and the system $2\text{LiBH}_4\text{-MgH}_2$ is considered for practical applications.¹⁸⁻²¹ The alkali earth metal borohydrides $\text{Mg}(\text{BH}_4)_2$ and $\text{Ca}(\text{BH}_4)_2$, have been studied to a great extent due to their high hydrogen content, rich structural polymorphism and some degree of reversibility.²²⁻²⁶ Recently, strontium borohydride was investigated but barium borohydride remain unknown, which has prompted the present investigation.²⁷ Here we report the synthesis, characterization and thermal decomposition of barium based borohydride chlorides prepared by mechanochemistry and investigated using *in situ* synchrotron radiation powder X-ray diffraction (SR-PXD), Fourier

transformed infrared spectroscopy (FT-IR) and simultaneous thermogravimetric analysis (TGA), differential scanning calorimetry (DSC), mass spectroscopy (MS) and temperature programmed photographic analysis (TPPA).

2 Experimental section

2.1 Synthesis

The samples in this work were prepared by high-energy mechanochemistry. Barium chloride, BaCl_2 (99.99 %, Sigma-Aldrich) and metal borohydrides, MBH_4 , $M = \text{Li, Na, or K}$ (>95.0 %, Sigma-Aldrich) were used as-received and mixed in molar ratios $\text{MBH}_4\text{-BaCl}_2$ of 2:1 or 1:1, see Table 1. The mixtures were ball milled in an 80 mL tungsten carbide steel container with 10 mm tungsten carbide balls, a sample to ball weight ratio of 1:35 using a Fritch Pulverisette No. 4. All samples were ball milled under the same conditions *i.e.* inert conditions (argon atmosphere) for a total of 2 h comprised of 2 minutes of milling each intervened by 2 minutes of pause to avoid sample heating.²⁸ A main disk speed of 400 rpm and a relative speed ratio of -2.25 were used for all samples. Preparation and manipulation of all the samples were performed in an argon-filled glove box with a circulation purifier, $p(\text{O}_2, \text{H}_2\text{O})$ below 1 ppm.

2.2 Synchrotron radiation powder X-ray diffraction

Time resolved *in-situ* synchrotron radiation powder X-ray diffraction (SR-PXD) data were measured at RT at the Swiss-Norwegian Beamlines (SNBL), BM01A, at the European Synchrotron Radiation Facility (ESRF) in Grenoble, France for the samples of $\text{LiBH}_4\text{-BaCl}_2$ in molar ratio of 2:1 and 1:1 using a wavelength of 0.8321 Å and for $\text{MBH}_4\text{-BaCl}_2$ ($M = \text{Li and Na}$) 2:1 using $\lambda = 0.7008$ Å. All data were collected using a MAR345 image plate detector (readout time of 83 s). The samples were typically mounted in glass capillaries (o.d. 0.5 mm) sealed with glue in an argon filled glovebox. A few experiments were conducted with samples mounted in quartz capillaries (o.d. 0.5 mm). For all experiments the capillaries were oscillated by 1°/s to reduce effects of preferred orientation during

X-ray exposure of 30 s. The samples were heated from RT to 300 or 400 °C at a heating rate of 5 °C/min. The temperature was controlled using an Oxford Cryostream 700+ or a Cyberstar hot air blower. The data were integrated using the Fit2D program.²⁹

2.3 Structure solution and Rietveld refinement

All Rietveld refinements were performed using the Fullprof program.³⁰ The backgrounds were described by linear interpolation between selected points, while pseudo-Voigt profile functions were used to fit the diffraction peaks. In general, unit cell parameters, zero shift, profile parameters and the overall temperature factors, B_{ov} were refined.

The structures of o -Ba(BH₄)_xCl_{2-x} and h -Ba(BH₄)_xCl_{2-x} were derived by Rietveld refinement starting from the structures of the orthorhombic polymorph of barium chloride, o -BaCl₂ ($Pnma$)³¹, and the hexagonal high temperature polymorph, h -BaCl₂ (space group $P-62m$)³², respectively. B-atoms were introduced on the Cl positions in the structural models of the relevant BaCl₂ polymorphs. Hydrogen atoms were not introduced in any of the structures due to the high scattering power of Ba. Thus the B-atoms were simply taken as the centre of the BH₄-anion. The positions and occupancies of B and Cl were refined, with the overall occupancy of B and Cl on each of the Cl-sites constrained to one. For both structures the refinement yielded B-occupancies on only one of the two Cl-sites while the other B-occupancy was approximately zero. Hence, these sites were regarded as BH₄-free. The final agreement factors for the refinements are listed with the Rietveld refinement profile in Figure S1 and S2. Note that due to the high scattering power of Ba compared to Cl and BH₄, the refined stoichiometry is less reliable and is thus only reported to the second decimal point.

2.4 Thermal analysis

Simultaneous thermogravimetric analysis (TGA), differential scanning calorimetry (DSC), and mass spectrometry (MS) were measured using a PerkinElmer STA 6000 apparatus connected to a Hiden Analytical HPR-20 QMS sampling system. The samples (1-5 mg) placed in an Al₂O₃ crucibles were

heated from RT to 500 °C ($\Delta T/\Delta t = 5$ °C/min) in argon flow of 65 mL/min. Mass spectroscopy was used to monitor the outlet gaseous species H_2 ($m/z = 2$) and B_2H_6 ($m/z = 27$).

2.5 Temperature programmed photographic analysis

Temperature programmed photographic analysis (TPPA) was performed using a previously described setup.³³ Photographs were collected using a digital camera while heating from RT to 400 °C with a heating rate of 5 °C/min. Samples (~10 mg) were loaded under argon in a glass vial and connected to an argon filled balloon to maintain an inert atmosphere. The glass vial was encased in an aluminum heating-block with open viewing windows for photography. A thermocouple was placed near the sample to monitor the temperature during heating.

2.6 Fourier transformed Infrared spectroscopy

Fourier transformed infrared spectroscopy (FT-IR) were recorded in transmission mode using a Nicolet 380 Avatar FT-IR spectrometer in the scanning range of 4000-400 cm^{-1} with a resolution of 4 cm^{-1} . A total of 32 scans were collected. The samples were placed directly on the infrared source and covered by a tight screw. This approach limited air exposure of the sample to a few seconds prior to the FT-IR measurement.

3 Results and discussion

3.1 Synthesis and initial phase analysis

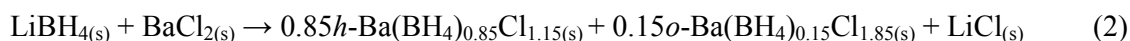
SR-PXD data measured at RT for the ball milled sample $LiBH_4$ - $BaCl_2$ (2:1) shows three sets of Bragg diffraction peaks, which are assigned to a new barium borohydride chloride, $Ba(BH_4)_xCl_{2-x}$, $LiCl$ and an unidentified compound, denoted **1** (see Figure 1 and Table 1). Only weak reflections are observed from the latter (strongest peak at $2\theta = 10.8^\circ$). The new barium borohydride chloride, $Ba(BH_4)_xCl_{2-x}$ is derived from the hexagonal high temperature polymorph of h - $BaCl_2$ (space group $P-62m$), and is henceforth denoted h - $Ba(BH_4)_xCl_{2-x}$. The structural similarity to h - $BaCl_2$ suggests, that mechano-chemical treatment and excess $LiBH_4$ facilitates anion substitution of large amounts of

BH₄ for Cl in the structure of the reactant, *o*-BaCl₂, and that the incorporation of the larger BH₄⁻ anion in the structure of *o*-BaCl₂ facilitates a structural transformation to a new compound *h*-Ba(BH₄)_xCl_{2-x}. The molar ratio of the formed *h*-Ba(BH₄)_xCl_{2-x} and LiCl is approximately 1:1 (49 and 51 mol%, respectively) and suggest the idealised composition, *h*-Ba(BH₄)Cl, see reaction scheme 1.



However, Rietveld refinement indicate that the anion substitution reaction is incomplete, *i.e.* a composition of *h*-Ba(BH₄)_{0.85}Cl_{1.15} possibly with remaining X-ray amorphous LiBH₄ in the reaction product supported by observation of FT-IR bands at 1080, 1220, 1270 cm⁻¹ of LiBH₄-BaCl₂ (2:1) and a reference sample of LiBH₄ (see Figure 2). The FT-IR data shows additional bands at 1160 cm⁻¹ for the ball-milled samples. These bands are similar to those observed for Ca(BH₄)₂,^{34, 35} and confirms the formation of a new alkaline earth borohydride. Furthermore, relatively strong IR absorption bands are observed at 700-400 cm⁻¹.

A more complex mixture of crystalline reaction products is observed by SR-PXD measured at *RT* for the mechano-chemically treated sample LiBH₄-BaCl₂ (1:1). Bragg diffraction peaks corresponding to two barium borohydride chlorides, *h*-Ba(BH₄)_{0.86}Cl_{1.14} (space group *P*-62*m*) and *o*-Ba(BH₄)_{0.16}Cl_{1.84} (space group *Pnma*) are observed along with LiCl, and weak diffraction from **1** (see Table 1 and Figure 1). This suggests a mechanism for anion substitution in the system LiBH₄-BaCl₂. Initially, *o*-BaCl₂ transforms to *o*-Ba(BH₄)_xCl_{2-x} with maximum of *x* ~ 0.15 and continued anion substitution in *o*-Ba(BH₄)_{0.15}Cl_{1.85} leads to a phase transformation to the hexagonal barium borohydride *h*-Ba(BH₄)_xCl_{2-x}, which accommodate higher amounts of borohydride, possibly *x* ~ 0.85. Thus, two solid solutions are in equilibrium during mechano-chemical treatment of sample LiBH₄-BaCl₂ (1:1), described by the idealised reaction scheme (2).



This suggest that the amount of LiBH_4 in sample $\text{LiBH}_4\text{-BaCl}_2$ (1:1) is limiting the reaction to (2) in contrast to sample $\text{LiBH}_4\text{-BaCl}_2$ (2:1) where excess LiBH_4 allow conversion of all $o\text{-Ba}(\text{BH}_4)_{0.15}\text{Cl}_{1.85}$ to $h\text{-Ba}(\text{BH}_4)_{0.85}\text{Cl}_{1.15}$ described by the idealised reaction scheme (1).

However, remaining (X-ray amorphous) LiBH_4 is also observed by FT-IR (Figure 2) for sample $\text{LiBH}_4\text{-BaCl}_2$ (1:1), which also confirms the formation of the new metal borohydride, similar to that in the ball milled sample of $\text{LiBH}_4\text{-BaCl}_2$ (2:1). The unidentified compound **1** observed in both samples (but not in any of the samples $\text{MBH}_4\text{-BaCl}_2$, $M = \text{Na}$ or K) might be a new lithium barium borohydride or a lithium barium borohydride chloride. Unfortunately, the observed diffraction from **1** is too weak to allow a reliably indexation.

For the samples $\text{MBH}_4\text{-BaCl}_2$, $M = \text{Na}$ or K (1:1) and (2:1), the reactants MBH_4 ($M = \text{Na}$ or K) and $o\text{-BaCl}_2$ are observed in the SR-PXD data obtained at RT after mechano-chemical treatment. However, detailed inspection of the SR-PXD data suggests substitution of smaller amounts of BH_4 in $o\text{-BaCl}_2$ as listed in Table 1. For the samples of $\text{NaBH}_4\text{-BaCl}_2$ in molar ratio 2:1 and 1:1 the compositions of the barium based solid solutions are found to be $o\text{-Ba}(\text{BH}_4)_{0.11}\text{Cl}_{1.89}$ and $o\text{-Ba}(\text{BH}_4)_{0.07}\text{Cl}_{1.93}$, respectively. Formation of sodium borohydride solid solutions $\text{Na}(\text{BH}_4)_{1-x}\text{Cl}_x$ with $x = 0.07$ are also suggested by Rietveld refinements for both samples of $\text{NaBH}_4\text{-BaCl}_2$. Full solubility in the system $\text{NaBH}_4\text{-NaCl}$ has previously been described possibly because both compounds have the rock salt structure.^{36, 37} For the samples of $\text{KBH}_4\text{-BaCl}_2$ the compositions of the solid solutions $\text{Ba}(\text{BH}_4)_x\text{Cl}_{2-x}$ are found to be $o\text{-Ba}(\text{BH}_4)_{0.12}\text{Cl}_{1.8}$ and $o\text{-Ba}(\text{BH}_4)_{0.09}\text{Cl}_{1.91}$, for the 2:1 and 1:1 sample, respectively. In this work, chloride substitution in KBH_4 appears not to take place, but was previously observed in the system $\text{KBH}_4\text{-KCl}$ at $T > \sim 230$ °C.³⁸

3.2 Crystal structures of barium borohydride chlorides

The structures of the two barium borohydride chlorides with idealised compositions, $o\text{-Ba}(\text{BH}_4)_{0.15}\text{Cl}_{1.85}$ and $h\text{-Ba}(\text{BH}_4)_{0.85}\text{Cl}_{1.15}$ formed by mechano-chemical synthesis of $\text{LiBH}_4\text{-BaCl}_2$

1:1 and 2:1, respectively, are investigated. The orthorhombic o -Ba(BH₄)_{0.15}Cl_{1.85} crystallizes in space group $Pnma$ (Table 2) and is derived from the RT orthorhombic polymorph of o -BaCl₂ (PbCl₂ structure type).³¹ The hexagonal h -Ba(BH₄)_{0.85}Cl_{1.15} crystallizes in space group $P-62m$ (Table 2) and is derived from the hexagonal high temperature polymorph h -BaCl₂ (anti-Fe₂P structure type).³² Both o - and h -Ba(BH₄) _{x} Cl_{2- x} exhibit partly ordered structures with one anionic site fully occupied by Cl anions and one site occupied by a statistical mixture of BH₄ and Cl anions. The unit cell volume (V) per formula unit (Z), V/Z is significantly larger for o -Ba(BH₄)_{0.15}Cl_{1.85} as compared to o -BaCl₂. The V/Z ratio for h -Ba(BH₄)_{0.85}Cl_{1.15} at RT is also significantly higher as compared to h -BaCl₂ (measured at 150 °C), see Table 2. This is due to significant difference in ionic radii of the anions, $r(\text{BH}_4^-) = 2.03 \text{ \AA}$ and $r(\text{Cl}^-) = 1.81 \text{ \AA}$.³⁹ Hence, incorporation of borohydride lead to structural expansion and a phase transformation of o -Ba(BH₄)_{0.15}Cl_{1.85} to h -Ba(BH₄)_{0.85}Cl_{1.15}. Thus, the anion substitution in o -BaCl₂ and transformation to h -BaCl₂ is comparable to thermal expansion. Interestingly, three Cl-free Ba(BH₄)₂ polymorphs have been reported (space groups $Pnmm$, $Pbcn$ and $P4_12_12_1$),⁴⁰ however no further details about their structure or information about their preparation have been published.

The structure of o -Ba(BH₄)_{0.15}Cl_{1.85} is built from Ba atoms coordinated to BH₄ and Cl in a tri-capped trigonal prism geometry (Figure 3, right). Four BH₄/Cl sites and two Cl atoms form the trigonal prism, with two sides capped by Cl atoms and one by coordination to a BH₄/Cl site. The Cl atoms are coordinated tetrahedrally by four Ba atoms, while another crystallographic anion position is populated by a statistical mixture of BH₄/Cl with a square pyramidal coordination to five Ba atoms.

The structure of h -Ba(BH₄)_{0.85}Cl_{1.15} consist of Ba1 tri-capped trigonal prism built from six Cl atoms and three BH₄/Cl sites. The Cl sites form the trigonal prism with each side capped by the coordination to the BH₄/Cl site, see Figure 3, left. The Ba2 trigonal prism is made by BH₄/Cl sites with each side capped by the coordination to three Cl atoms. The BH₄/Cl sites are positioned in a

square pyramidal coordination by five Ba atoms, while four Ba atoms coordinate the Cl atoms tetrahedrally, similar to the o -Ba(BH₄)_{0.15}Cl_{1.85} structure.

Interestingly, borohydride complexes are placed at the square pyramidal crystallographic site with coordination to five Ba, whereas no BH₄ substitution is observed on the Cl site with tetrahedral coordination, observed for both h -Ba(BH₄)_{0.85}Cl_{1.15} and o -Ba(BH₄)_{0.15}Cl_{1.85}. This might be explained by comparing Ba-Cl bonding distances in the two BaCl₂ polymorphs. The square pyramidal anion site appears to be larger and therefore better able accommodate the larger BH₄ complex anion. This is illustrated by the Ba-Cl distances in the range 3.18 to 3.58 Å and 2.86 to 3.17 Å at RT for o -BaCl₂³¹ and 3.29 to 3.40 Å and 3.06 to 3.13 Å at 150 °C for h -BaCl₂ for the square pyramidal and tetrahedral coordination, respectively.³² Hence, the tetrahedral Cl site might be too small to accommodate the larger BH₄ units.

The new hexagonal barium borohydride chloride, h -Ba(BH₄)_{0.85}Cl_{1.15}, transforms to another orthorhombic compound o -Ba(BH₄)_{0.85}Cl_{1.15} upon heating to ~200 °C. This structure of o -Ba(BH₄)_{0.85}Cl_{1.15} is derived from the orthorhombic BaBr₂, o -BaBr₂ (space group *Pnma*, *Z*=4, PbCl₂ structure type), and simply entails an expansion and distortion of the orthorhombic o -Ba(BH₄)_{0.16}Cl_{1.84} observed at RT (which were more closely related to o -BaCl₂). The structure of o -Ba(BH₄)_{0.85}Cl_{1.15} observed at 200 °C consists of a hexagonal close packed (h.c.p.) array of Ba cations with the tetrahedral interstices occupied by two symmetrically independent Br anions. However, displacement of the ions from idealized position results in a distorted 9-fold tricapped trigonal coordination of the Ba cation.⁴¹ Unit cell dimension and volume for o -Ba(BH₄)_{0.85}Cl_{1.15}, o -BaCl₂ and o -BaBr₂ are given in Table 2.

3.3 Thermal behaviour of barium borohydride chlorides

Thermal decomposition of o - and h -Ba(BH₄)_{*x*}Cl_{2-*x*} was investigated by thermal analysis, *i.e.* TGA-DSC-MS, TPPA and *in situ* SR-PXD for the ball milled sample of LiBH₄-BaCl₂ in molar ratio 2:1.

3.3.1 *In situ* SR-PXD of barium borohydrides

In situ time resolved synchrotron radiation powder X-ray diffraction (SR-PXD) is measured for the sample $\text{LiBH}_4\text{-BaCl}_2$ (2:1) from *RT* to 300 °C ($\Delta T/\Delta t = 5$ °C/min), see Figure 4. The first diffraction patterns measured at *RT* shows three sets of Bragg diffraction peaks indexed as *h*- $\text{Ba}(\text{BH}_4)_{0.85}\text{Cl}_{1.15}$, LiCl and small amounts of the unknown compound **1**. At ~125 °C, all diffraction from **1** vanishes, which causes no visible change in the diffraction from the other components of the sample $\text{Ba}(\text{BH}_4)_x\text{Cl}_{2-x}$ and LiCl or formation of decomposition products. The relatively low decomposition temperature may indicate that **1** is a new lithium barium borohydride as borohydrides are in general less thermally stable than *e.g.* oxides or chlorides.

Upon further heating to ~200 °C, *h*- $\text{Ba}(\text{BH}_4)_{0.85}\text{Cl}_{1.15}$, transforms to a new orthorhombic barium borohydride chloride compound, *o*- $\text{Ba}(\text{BH}_4)_{0.85}\text{Cl}_{1.15}$, clearly recognized in the SR-PXD (Figure 4). The composition of *o*- $\text{Ba}(\text{BH}_4)_{0.85}\text{Cl}_{1.15}$ and *h*- $\text{Ba}(\text{BH}_4)_{0.85}\text{Cl}_{1.15}$ does not change significantly during heating in the temperature range *RT* to 300 °C, *i.e.* no significant BH_4^- or Cl^- substitution is observed. The unit cell parameters for *o*- $\text{Ba}(\text{BH}_4)_{0.85}\text{Cl}_{1.15}$ at ~200 °C, $a = 8.3659(6)$, $b = 4.8731(3)$ and $c = 9.6898(7)$ Å, are similar to those of the orthorhombic BaBr_2 polymorph *o*- BaBr_2 , $a = 8.2746(1)$, $b = 4.9599(1)$ and $c = 9.9264(2)$ Å.⁴⁰ Hence the structural transformation from *h*- to *o*- $\text{Ba}(\text{BH}_4)_{0.85}\text{Cl}_{1.15}$ might be caused by the thermal expansion increasing the average size of the thermal vibration ellipsoids of BH_4^- and Cl^- towards that of Br^- . Thus, thermal treatment at $T > 200$ °C allow higher degree of anion substitution in the orthorhombic barium borohydride structure as compared to mechano-chemical treatment, which formed *o*- $\text{Ba}(\text{BH}_4)_{0.15}\text{Cl}_{1.85}$. At ~290 °C, the experiment was stopped due to breakage of the glass capillary, which occurred at approximately the same temperature for several measurements. This may be due to a reaction between the glass capillary and molten LiBH_4 ,⁴² possibly present in an X-ray amorphous state. Therefore, *in situ* SR-PXD experiments were also conducted with samples mounted in sapphire capillaries.⁴³ Further

experimental studies indicated that $o\text{-Ba}(\text{BH}_4)_{0.85}\text{Cl}_{1.15}$ is stable up to 500 °C, however the data quality did not allow for determination of the exact composition and unit cell parameters.

For the ball-milled sample $\text{NaBH}_4\text{-BaCl}_2$ (2:1) *in situ* SR-PXD measurements reveal two anion substitution reactions during heating, *i.e.* BH_4^- and Cl^- are substituted into $o\text{-BaCl}_2$ and NaBH_4 , respectively, see Figure S4 and S5. This results in formation of two solid solutions according to reaction scheme 3.



To follow this reaction in more detail the unit cell parameters of the two solid solutions were extracted by Rietveld refinement of the SR-PXD data measured from RT to 400 °C (Figure 5). The double anion substitution reaction is initiated at $T \sim 260$ °C, where a decrease in the unit cell parameter for $\text{Na}(\text{BH}_4)_{1-x}\text{Cl}_x$ is observed simultaneously with an increase in the unit cell parameters of $o\text{-Ba}(\text{BH}_4)_x\text{Cl}_{2-x}$ beyond that resulting from thermal expansion. Thus, the reaction occur with NaCl as an intermediate compound, which is immediately dissolved in remaining NaBH_4 forming the solid solution $\text{Na}(\text{BH}_4)_{1-x}\text{Cl}_x$. In the temperature range from ~ 310 to 380 °C, the reactions seems to proceed at a slower rate, *i.e.* the unit cell parameter for $\text{Na}(\text{BH}_4)_{1-x}\text{Cl}_x$ does not change significantly, which means that Cl^- is still substituted into the structure when taken the expected thermal expansion into account. Furthermore, the a -axis for $\text{Ba}(\text{BH}_4)_x\text{Cl}_{2-x}$ expands significantly in this temperature range ~ 300 °C to 360 °C suggesting that BH_4^- substitution into the other Cl site might occur in this temperature range. Upon further heating all cell parameters are observed to decrease. This is likely due to initiated decomposition of the borohydride entailed in the solid solutions. However, no decomposition products were observed in the temperature range of these measurements up to 400 °C.

Unit cell parameters for the solid solutions of $o\text{-Ba}(\text{BH}_4)_{0.11}\text{Cl}_{1.89}$ and $\text{Na}(\text{BH}_4)_{0.93}\text{Cl}_{0.07}$ as a function of temperature is provided in Figure 5. The data is extracted by Rietveld refinement of *in situ* SR-PXD data measured for ball-milled $\text{NaBH}_4\text{-BaCl}_2$ (2:1) shown in Figure S3. The linear thermal

expansion coefficient, α_L , based on the data from RT to 270 °C and calculated from the equation: $\alpha_L = (1/L_0)(\Delta L/\Delta T)$ (L = unit cell axis or volume, L_0 = extrapolated value at $T=0$ °C) are $\alpha_a = 4.20 \cdot 10^{-5} \text{ K}^{-1}$, $\alpha_b = 4.45 \cdot 10^{-5} \text{ K}^{-1}$, $\alpha_c = 2.23 \cdot 10^{-5} \text{ K}^{-1}$, $\alpha_{\text{volume}} = 1.11 \cdot 10^{-4} \text{ K}^{-1}$ for $\text{Ba}(\text{BH}_4)_x\text{Cl}_{2-x}$ and $\alpha_a = 8.95 \cdot 10^{-2} \text{ K}^{-1}$, $\alpha_{\text{volume}} = 2.27 \cdot 10^{-4} \text{ K}^{-1}$ for $\text{Na}(\text{BH}_4)_x\text{Cl}_{1-x}$ which is closer to the thermal expansion reported for NaCl ($2.562(6) \cdot 10^{-4} \text{ K}^{-1}$), than that of NaBH_4 ($5.36(6) \cdot 10^{-4} \text{ K}^{-1}$).³⁶³⁶

3.3.2 Thermal analysis of barium borohydride chlorides

Simultaneous thermogravimetric analysis (TGA), differential scanning calorimetry (DSC) and mass spectroscopy (MS) data is shown in Figure 6 while Figure 7 displays selected photos from the temperature programmed photographic analysis (TPPA) of the mechano-chemically treated sample $\text{LiBH}_4\text{-BaCl}_2$ (2:1). A mass loss of ~3.0 wt.% occurs at a steady rate in the temperature range 200 to 400 °C. Upon further heating the rate of the mass loss increases and a total mass loss of ~5.3 wt% is observed in the temperature range 200 to 500 °C. The calculated hydrogen content of the sample $\text{LiBH}_4\text{-BaCl}_2$ (2:1) is 3.2 wt.% for the sample. The increased rate of mass loss corresponds well to the observations by MS where H_2 is released above 400 °C. This H_2 release is assigned to decomposition of the amorphous LiBH_4 present in the sample. At 240 °C, a minor release of H_2 is observed by MS. DSC data reveal a minor endothermic event at 205 °C, which may be assigned to transformation of $h\text{-Ba}(\text{BH}_4)_{0.85}\text{Cl}_{1.15}$ to $o\text{-Ba}(\text{BH}_4)_{0.85}\text{Cl}_{1.15}$, clearly recognized in the SR-PXD (Figure 6).

In the DSC data a small broad endothermic signal is observed between 400 and 500 °C corresponding well with the large mass loss. Furthermore, small endothermic signals are observed at 97, 205, and 250 °C. At the latter temperature a slight change of colour from white to light brown is observed by TPPA. The colour of the powder gradually turns darker until the sample melts at ca. 400 °C. Release of gas is visually observed (see Figure 4b). No Release of B_2H_6 is observed, thus boron likely remains in the solid state.

4 Conclusion

The synthesis, mechanism of formation, crystal structure, and thermal decomposition has been investigated for three novel barium borohydride chlorides. The compounds were obtained by a mechano-chemical reaction of LiBH_4 and BaCl_2 .

Firstly, the orthorhombic barium chloride, $o\text{-BaCl}_2$ transforms to $o\text{-Ba}(\text{BH}_4)_x\text{Cl}_{2-x}$, $x \sim 0.15$. Additional LiBH_4 in the reaction mixture leads to continued anion substitution and to a phase transformation from $o\text{-Ba}(\text{BH}_4)_x\text{Cl}_{2-x}$ to hexagonal barium borohydride chloride, $h\text{-Ba}(\text{BH}_4)_x\text{Cl}_{2-x}$, $x \sim 0.85$, which closely resembles $h\text{-BaCl}_2$. The structure of both $o\text{-}$ and $h\text{-Ba}(\text{BH}_4)_x\text{Cl}_{2-x}$ is partly ordered with one anionic site fully occupied by Cl anions and one site occupied by a mixture of BH_4 and Cl anions. Remarkably, the borohydride complexes are only placed at the square pyramidal crystallographic site with coordination to five Ba, while no BH_4 substitution is observed on the Cl site with tetrahedral coordination. This is observed for both $h\text{-Ba}(\text{BH}_4)_{0.85}\text{Cl}_{1.15}$ and $o\text{-Ba}(\text{BH}_4)_{0.15}\text{Cl}_{1.85}$ implying BH_4 units are too large to be accommodated by the smaller tetrahedral Cl site.

Investigation of the thermal decomposition by *in situ* SR-PXD and coupled TGA-DSC-MS showed that at $T > \sim 200$ °C, $h\text{-Ba}(\text{BH}_4)_{0.85}\text{Cl}_{1.15}$ transforms to another new orthorhombic barium borohydride chloride compound, $o\text{-Ba}(\text{BH}_4)_{0.85}\text{Cl}_{1.15}$, which is related to orthorhombic BaBr_2 , $o\text{-BaBr}_2$ (space group $Pnma$, $Z=4$) and consists of a hexagonal close packed (h.c.p.) array of Ba cations with the tetrahedral interstices occupied by two symmetrically independent Br anions. However, displacement of the ions from idealized position results in a distorted 9-fold tricapped trigonal coordination of the Ba cation

References

1. D. J. C. McKay, *Sustainable energy – with out hot air*, UTH Cambridge, 2009.
2. M. B. Ley, L. H. Jepsen, Y.-S. Lee, Y. W. Cho, J. M. Bellosta von Colbe, M. Dornheim, M. Rokni, J. O. Jensen, M. Sloth, Y. Filinchuk, J. E. Jørgensen, F. Besenbacher and T. R. Jensen, *Mater. Today*, 2014, **17**, 122-128.
3. M. Felderhoff, C. Weidenthaler, R. von Helmolt and U. Eberle, *Phys. Chem. Chem. Phys.*, 2007, **9**, 2643-2653.
4. L. H. Jepsen, M. B. Ley, Y.-S. Lee, Y. W. Cho, M. Dornheim, J. O. Jensen, Y. Filinchuk, J. E. Jørgensen, F. Besenbacher and T. R. Jensen, *Mater. Today*, 2014, **17**, 129-135.
5. L. H. Rude, T. K. Nielsen, D. B. Ravnsbæk, U. Bösenberg, M. B. Ley, B. Richter, L. M. Arnbjerg, M. Dornheim, Y. Filinchuk, F. Besenbacher and T. R. Jensen, *Phys. Status Solidi A*, 2011, **208**, 1754-1773.
6. D. B. Ravnsbæk, Y. Filinchuk, R. Cerny and T. R. Jensen, *Z. Krist.*, 2010, **225**, 557-569.
7. S.-i. Orimo, Y. Nakamori, J. R. Eliseo, A. Züttel and C. M. Jensen, *Chem. Rev.*, 2007, **107**, 4111-4132.
8. Q. Lai, M. Paskevicius, D. A. Sheppard, C. E. Buckley, A. W. Thornton, M. R. Hill, Q. Gu, J. Mao, Z. Huang, H. K. Liu, Z. Guo, A. Banerjee, S. Chakraborty, R. Ahuja and K.-F. Aguey-Zinsou, *ChemSusChem*, 2015.
9. P. Schouwink, M. B. Ley, A. Tissot, H. Hagemann, T. R. Jensen, L. Smrčok and R. Černý, *Nat Commun*, 2014, **5**, 5706-5701-5706-5710.
10. P. Schouwink, V. D'Anna, M. B. Ley, L. M. Lawson Daku, B. Richter, T. R. Jensen, H. Hagemann and R. Černý, *J. Phys. Chem. C*, 2012, **116**, 10829-10840.
11. Y. Sadikin, K. Stare, P. Schouwink, M. Brix Ley, T. R. Jensen, A. Meden and R. Černý, *J. Solid State Chem.*, 2015, **225**, 231-239.
12. R. Černý, P. Schouwink, Y. Sadikin, K. Stare, L. u. Smrčok, B. Richter and T. R. Jensen, *Inorg. Chem.*, 2013, **52**, 9941-9947.
13. H. W. Li, Y. Yan, S. Orimo, A. Züttel and C. M. Jensen, *Energies*, 2011, **4**, 185-214.
14. M. B. Ley, D. B. Ravnsbæk, Y. Filinchuk, Y.-S. Lee, R. Janot, Y. W. Cho, J. Skibsted and T. R. Jensen, *Chem. Mater.*, 2012, **24**, 1654-1663.
15. M. B. Ley, S. Boulineau, R. Janot, Y. Filinchuk and T. R. Jensen, *J. Phys. Chem. C*, 2012, **116**, 21267-21276.
16. B. Richter, D. B. Ravnsbaek, N. Tumanov, Y. Filinchuk and T. R. Jensen, *Dalton Trans.*, 2015, **44**, 3988-3996.
17. Y. Filinchuk, B. Richter, T. R. Jensen, V. Dmitriev, D. Chernyshov and H. Hagemann, *Angew. Chem. Int. Ed.*, 2011, **50**, 11162-11166.
18. U. Bösenberg, J. W. Kim, D. Gossler, N. Eigen, T. R. Jensen, J. M. B. von Colbe, Y. Zhou, M. Dahms, D. H. Kim, R. Günther, Y. W. Cho, K. H. Oh, T. Klassen, R. Bormann and M. Dornheim, *Acta Mater.*, 2010, **58**, 3381-3389.
19. U. Bösenberg, S. Doppiu, L. Mosegaard, G. Barkhordarian, N. Eigen, A. Borgschulte, T. R. Jensen, Y. Cerenius, O. Gutfleisch, T. Klassen, M. Dornheim and R. Bormann, *Acta Mater.*, 2007, **55**, 3951-3958.
20. J. J. Vajo, S. L. Skeith and F. Mertens, *J. Phys. Chem. B*, 2005, **109**, 3719-3722.
21. Y. W. Cho, J.-H. Shim and B.-J. Lee, *Calphad*, 2006, **30**, 65-69.
22. G. Severa, E. Ronnebro and C. M. Jensen, *Chem. Commun.*, 2010, **46**, 421-423.
23. G. L. Soloveichik, Y. Gao, J. Rijssenbeek, M. Andrus, S. Kniajanski, R. C. Bowman, S.-J. Hwang and J.-C. Zhao, *Int. J. Hydrogen Energy*, 2009, **34**, 916-928.
24. T. Matsunaga, F. Buchter, P. Mauron, M. Bielman, Y. Nakamori, S. Orimo, N. Ohba, K. Miwa, S. Towata and A. Züttel, *J. Alloys Compd.*, 2008, **459**, 583-588.

25. S. Sartori, K. D. Knudsen, Z. Zhao-Karger, E. G. Bardajj, M. Fichtner and B. C. Hauback, *Nanotechnology*, 2009, **20**, 505702.
26. M. Aoki, K. Miwa, T. Noritake, N. Ohba, M. Matsumoto, H. W. Li, Y. Nakamori, S. Towata and S. Orimo, *Appl. Phys. A*, 2008, **92**, 601-605.
27. D. B. Ravnsbæk, E. A. Nickels, R. Černý, C. H. Olesen, W. I. F. David, P. P. Edwards, Y. Filinchuk and T. R. Jensen, *Inorg. Chem.*, 2013, **52**, 10877-10885.
28. J. Huot, D. B. Ravnsbæk, J. Zhang, F. Cuevas, M. Latroche and T. R. Jensen, *Prog. Mater. Sci.*, 2013, **58**, 30-75.
29. A. P. Hammersley, S. O. Svensson, M. Hanfland, A. N. Fitch and D. Hausermann, *High Pressure Res.*, 1996, **14**, 235-248.
30. J. Rodríguez-Carvajal, *Physica B*, 1993, **192**, 55-69.
31. E. B. Brackett, T. E. Brackett and R. L. Sass, *J. Phys. Chem.*, 1963, **67**, 2132-2135.
32. A. Haase and G. Brauer, *Z. Anorg. Allg. Chem.*, 1978, **441**, 181-195.
33. M. Paskevicius, M. B. Ley, D. A. Sheppard, T. R. Jensen and C. E. Buckley, *Phys. Chem. Chem. Phys.*, 2013, **15**, 19774-19789.
34. V. D'Anna, A. Spyratou, M. Sharma and H. Hagemann, *Spectrochim Acta A Mol Biomol Spectrosc.*, 2014, **128**, 902-906.
35. A. Liu, S. Xie, S. Dabiran-Zohoori and Y. Song, *J. Phys. Chem. C*, 2010, **114**, 11635-11642.
36. D. B. Ravnsbæk, L. H. Rude and T. R. Jensen, *J. Solid State Chem.*, 2011, **184**, 1858-1866.
37. I. Llamas-Jansa, N. Aliouane, S. Deledda, J. E. Fonnelop, C. Frommen, T. Humphries, K. Lieutenant, S. Sartori, M. H. Sørby and B. C. Hauback, *J. Alloy Compd*, 2012, **530**, 186-192.
38. R. Cerny, D. B. Ravnsbæk, G. Severa, Y. Filinchuk, V. D' Anna, H. Hagemann, D. Haase, J. Skibsted, C. M. Jensen and T. R. Jensen, *J. Phys. Chem. C*, 2010, **114**, 19540-19549.
39. D. R. Lide, *CRC Handbook of Chemistry and Physics*, CRC Press, 88 edn., 2007.
40. R. Černý, P. Schouwink, *Acta Cryst.*, 2015, **B71**, 619-640.
41. S. Hull, S. T. Norberg, I. Ahmed, S. G. Eriksson and C. E. Mohn, *J. Solid State Chem.*, 2011, **184**, 2925-2935.
42. L. Mosegaard, B. Møller, J.-E. Jørgensen, Y. Filinchuk, Y. Cerenius, J. C. Hanson, E. Dimasi, F. Besenbacher and T. R. Jensen, *J. Phys. Chem. C*, 2008, **112**, 1299-1303.
43. B. R. S. Hansen, K. T. Møller, M. Paskevicius, A.-C. Dippel, P. Walter, C. J. Webb, C. Pistidda, N. Bergemann, M. Dornheim, T. Klassen, J.-E. Jørgensen and T. R. Jensen, *J. Appl. Cryst.*, 2015, **48**, 1234-1241.

Table 1. Reactant composition, molar ratios and reaction products observed by SR-PXD at *RT* after ball milling of samples.

Reactants	Composition	Reaction products*
LiBH ₄ –BaCl ₂ (2:1)	1.99:1.00	<i>h</i> -Ba(BH ₄) _{0.85} Cl _{1.15} (49 mol%), 1 , LiCl (51 mol%)
LiBH ₄ –BaCl ₂ (1:1)	1.00:1.00	<i>h</i> -Ba(BH ₄) _{0.86} Cl _{1.14} (4.7 mol%), <i>o</i> -Ba(BH ₄) _{0.16} Cl _{1.84} (44.3 mol%), 1 , LiCl (51.0 mol%)
NaBH ₄ –BaCl ₂ (2:1)	2.00:1:00	<i>o</i> -Ba(BH ₄) _{0.11} Cl _{1.89} (35.5 mol%), Na(BH ₄) _{0.93} Cl _{0.07} (64.7 mol%)
NaBH ₄ –BaCl ₂ (1:1)	1.00:1.00	<i>o</i> -Ba(BH ₄) _{0.07} Cl _{1.93} (54.5 mol%), Na(BH ₄) _{0.93} Cl _{0.07} (45.5 mol%)
KBH ₄ –BaCl ₂ (2:1)	2.00:1.00	<i>o</i> -Ba(BH ₄) _{0.12} Cl _{1.88} (66.2 mol%), KBH ₄ (33.8 mol%)
KBH ₄ –BaCl ₂ (1:1)	1.00:1.00	<i>o</i> -Ba(BH ₄) _{0.09} Cl _{1.91} (43.3 mol%), KBH ₄ (56.7 mol%)

*) The small amounts of **1** are neglected in the listed mol%.

Table 2. Comparison of unit cell parameters and volume per formula unit for the $\text{Ba}(\text{BH}_4)_{1-x}\text{Cl}_{1+x}$ structures and the room and high temperature BaCl_2 polymorphs, *o*- BaCl_2 and *h*- BaCl_2 .

	<i>o</i> - $\text{Ba}(\text{BH}_4)_{0.16}\text{Cl}_{1.84}$	<i>o</i> - BaCl_2	<i>h</i> - $\text{Ba}(\text{BH}_4)_{0.85}\text{Cl}_{1.15}$	<i>h</i> - BaCl_2	<i>o</i> - $\text{Ba}(\text{BH}_4)_{0.85}\text{Cl}_{1.15}$	<i>o</i> - BaBr_2
Space group	<i>Pnma</i>	<i>Pnma</i>	<i>P-62m</i>	<i>P-62m</i>	<i>Pnma</i>	<i>Pnma</i>
<i>a</i> (Å)	8.228(6)	7.865(8)	8.2945(3)	8.113(8)	8.3659(6)	8.2746(1)
<i>b</i> (Å)	4.785(3)	4.731(4)	8.2945(3)	8.113(8)	4.8731(3)	4.9599(1)
<i>c</i> (Å)	9.620(6)	9.421(8)	4.7776(3)	4.675(5)	9.6898(7)	9.9264(2)
Ba-(B/Cl) (Å)	3.3217(15)- 3.6352(14)	3.18-3.52	3.432(9)-3.567(8)	3.29-3.40	3.37(2)-3.70(3)	3.384- 3.828
Ba-Cl (Å)	3.0901(13)- 3.156(2)	2.86-3.17	3.163(7)-3.168(4)	3.06-3.13	3.171(13)-3.140(9)	3.212- 3.238
<i>Z</i>	4	4	3	3	4	4
<i>V</i> (Å ³)	378.749	350.549	284.656	266.486	395.03	407.39
<i>T</i> (°C)	<i>RT</i>	<i>RT</i>	<i>RT</i>	150	200	69
<i>V/Z</i> (Å ³)	94.68(9)	87.64(2)	96.89(2)	88.8(2)	98.76	101.84
ρ (g cm ⁻³)	3.59	3.94	3.27	3.89	3.21	4.78
ρ_v (H ₂) (kg H ₂ m ⁻³)	11.1	-	58.9	-	57.8	-
ρ_m (H ₂) (wt.%)	0.31	-	1.80	-	1.80	-

^aTemperature of PXD data collection

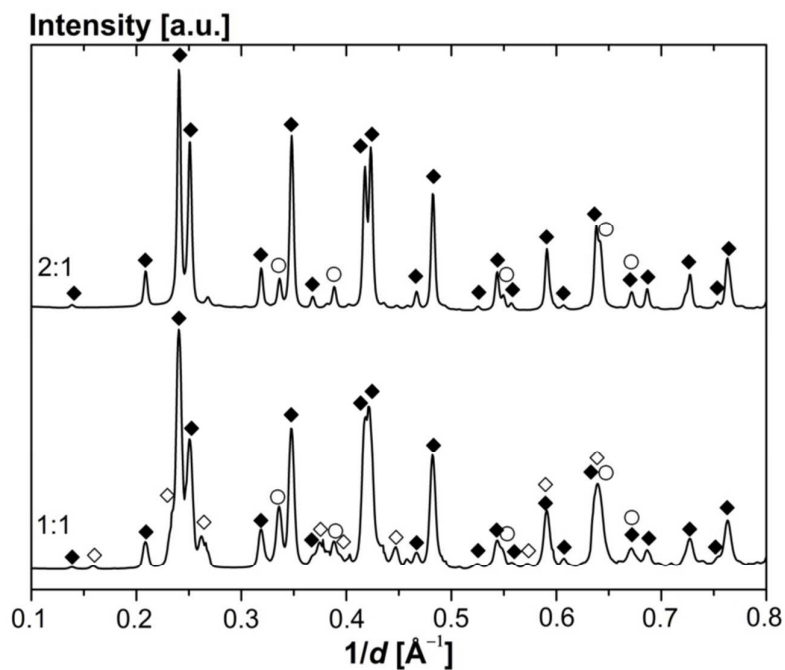


Figure 1. SR-PXD data measured at RT for a ball milled sample of LiBH₄-BaCl₂ in molar ratios 2:1 ($\lambda = 0.8321 \text{ \AA}$) and 1:1 ($\lambda = 0.700130 \text{ \AA}$), at BM01A, ESRF. Symbols: ◇ *o*-Ba(BH₄)_xCl_{2-x}, ◆ *h*-Ba(BH₄)_xCl_{2-x}, and ○ LiCl. Unmarked reflections correspond to the unknown compound denoted **1**.

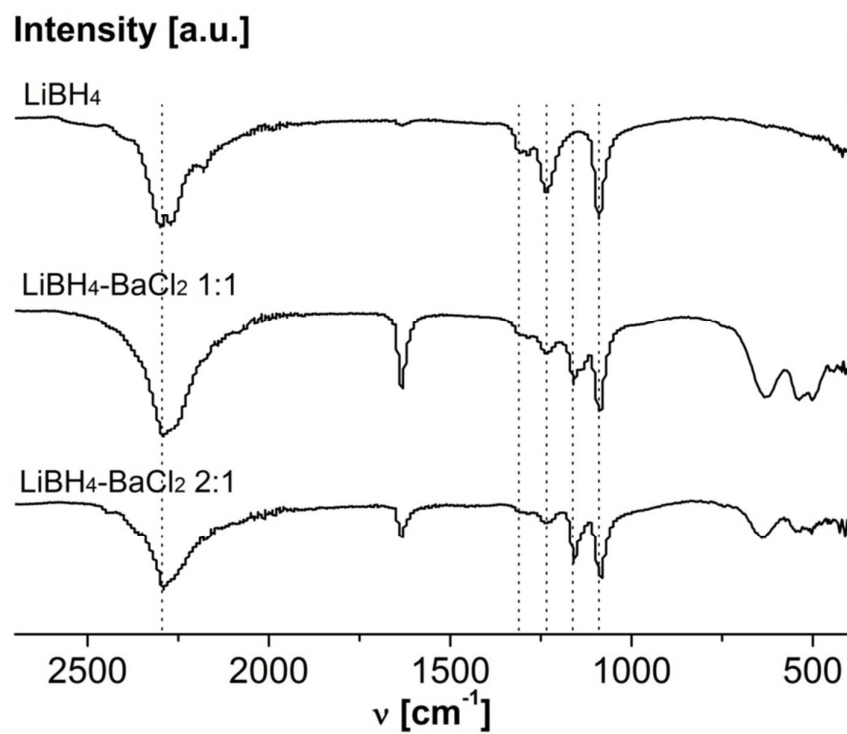


Figure 2. FT-IR spectra from 2700-400 cm^{-1} for LiBH_4 (top), $\text{LiBH}_4\text{-BaCl}_2$ 1:1 (middle), and $\text{LiBH}_4\text{-BaCl}_2$ 2:1 (bottom) showing B-H stretching ($\sim 2300 \text{ cm}^{-1}$), O-H bending (1700 cm^{-1}), B-H bending ($\sim 1200 \text{ cm}^{-1}$), and M-B lattice vibrations ($400\text{-}700 \text{ cm}^{-1}$).

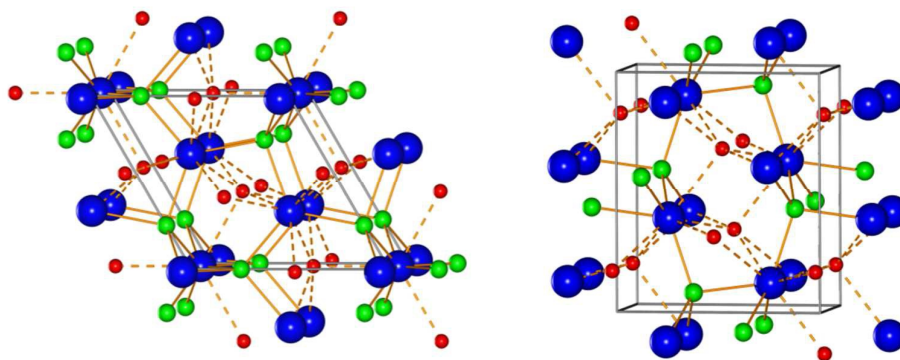


Figure 3. Crystal structures of $h\text{-Ba}(\text{BH}_4)_{0.85}\text{Cl}_{1.15}$ ($P-62m$) viewed approximately along the c -axis (left) and $o\text{-Ba}(\text{BH}_4)_{0.16}\text{Cl}_{1.84}$ ($Pnma$) approximately along the b -axis (right). Ba: blue, Cl: green, and B/Cl: red. The Ba-B coordination is shown as dashed lines. Hydrogen positions have not been determined for these structures.

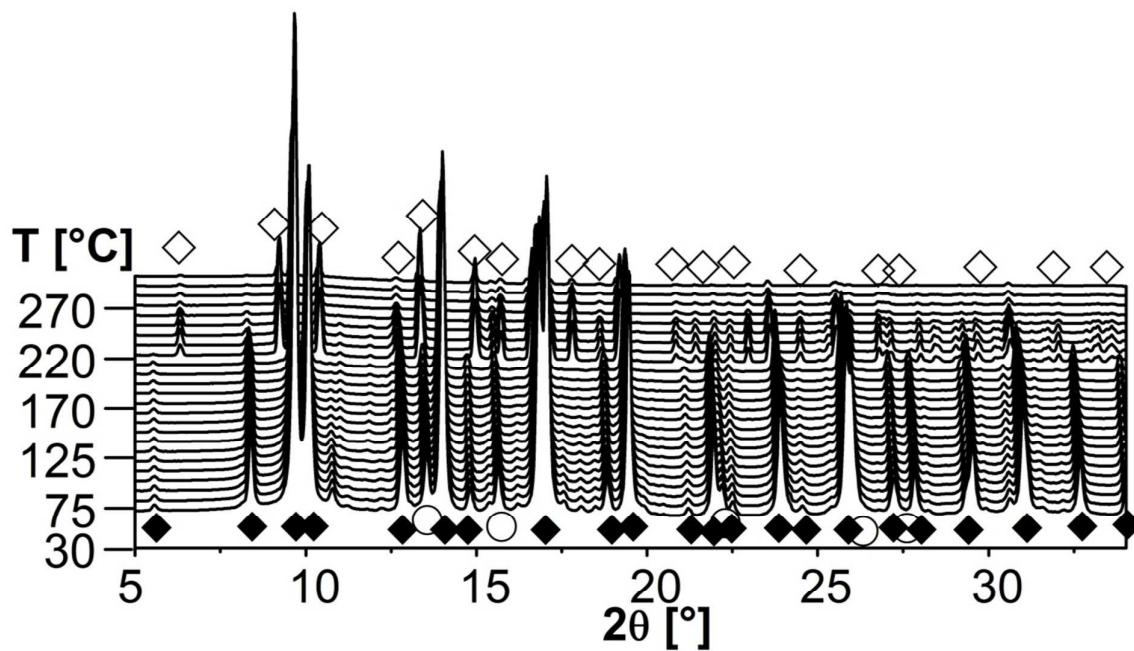


Figure 4. *In situ* SR-PXD data of a sample containing $h\text{-Ba}(\text{BH}_4)_{0.85}\text{Cl}_{1.15}$, **1**, LiCl (LiBH₄-BaCl₂, 2:1) measured from *RT* to 300 °C, $\Delta T/\Delta t = 5$ °C/min (BM01A, ESRF, $\lambda = 0.700818$ Å). Symbols: ◇ $o\text{-Ba}(\text{BH}_4)_x\text{Cl}_{2-x}$, ◆ $h\text{-Ba}(\text{BH}_4)_x\text{Cl}_{2-x}$, and ○ LiCl. Unmarked reflections correspond to the unknown compound denoted **1**.

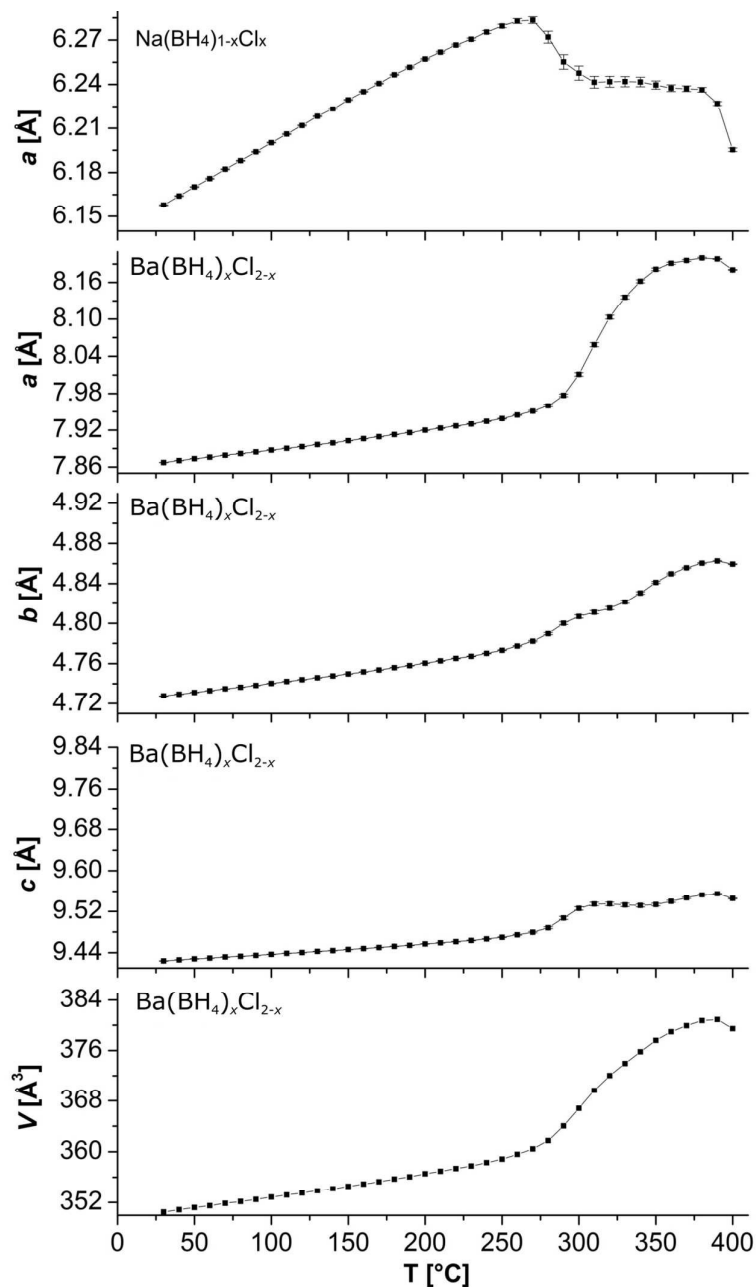


Figure 5. Unit cell parameters for the solid solutions of Ba(BH₄)_xCl_{2-x} and Na(BH₄)_{1-x}Cl_x as a function of temperature. The values are extracted based on Rietveld refinement of *in situ* SR-PXD data measured for a ball-milled sample of NaBH₄-BaCl₂ in molar ratio 2:1.

The linear thermal expansion coefficient, α_L , based on the data from RT to 270 °C and calculated

from the equation: $\alpha_L = (1/L_0)(\Delta L/\Delta T)$ (L = unit cell axis or volume, L_0 = extrapolated value at $T = 0$ °C) were $\alpha_a = 4.20 \cdot 10^{-5} \text{ K}^{-1}$, $\alpha_b = 4.45 \cdot 10^{-5} \text{ K}^{-1}$, $\alpha_c = 2.23 \cdot 10^{-5} \text{ K}^{-1}$, $\alpha_{\text{volume}} = 1.11 \cdot 10^{-4} \text{ K}^{-1}$ for $\text{Ba}(\text{BH}_4)_x\text{Cl}_{2-x}$ and $\alpha_a = 8.95 \cdot 10^{-2} \text{ K}^{-1}$, $\alpha_{\text{volume}} = 2.27 \cdot 10^{-4} \text{ K}^{-1}$.

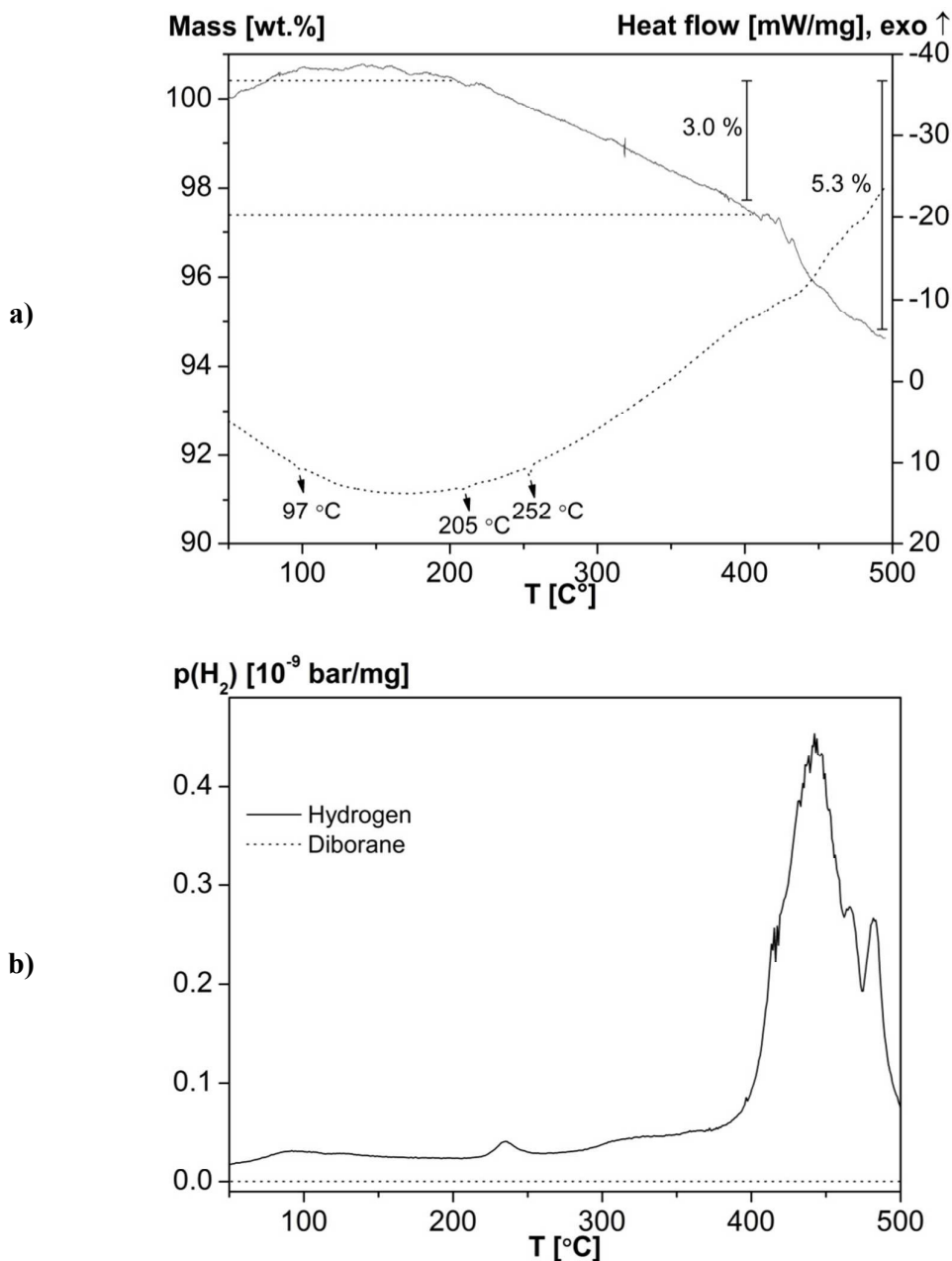


Figure 6. Simultaneous thermal analysis. **a)** TGA (black line) and DSC (grey line) measurement of $\text{LiBH}_4\text{-BaCl}_2$ 2:1 heated from RT to 500 °C ($\Delta T/\Delta t = 5$ °C/min, argon flow of 65 mL/min.). **b)** The MS signal of hydrogen ($m/z = 2$) accompanying the TGA-DSC measurement of $\text{LiBH}_4\text{-BaCl}_2$ 2:1 from RT to 500 °C ($\Delta T/\Delta t = 5$ °C/min, argon flow of 65 mL/min.). No diborane was detected during the experiment.

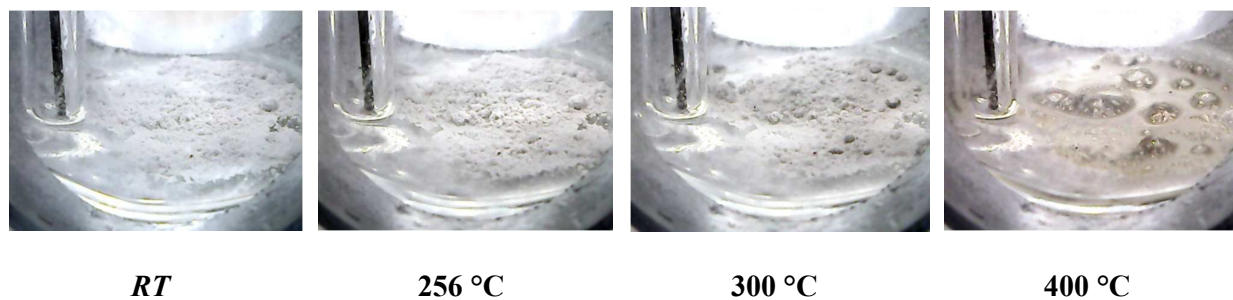
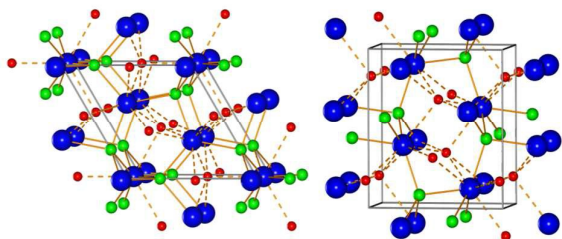


Figure 7. Selected photographs obtained by temperature programmed photographic analysis of the ball-milled sample $\text{LiBH}_4\text{-BaCl}_2$ (2:1) from *RT* to 400 °C ($\Delta T/\Delta t = 5$ °C/min).

Table of content entry:



A series of novel barium-based borohydrides, structurally resembling various BaCl_2 and BaBr_2 polymorphs, were prepared using mechanochemistry